EBE, an AP2/ERF Transcription Factor Highly Expressed in Proliferating Cells, Affects Shoot Architecture in Arabidopsis[W]

Mohammad Mehrnia, Salma Balazadeh, María-Inés Zanor[1], and Bernd Mueller-Roeber*

Max-Planck Institute of Molecular Plant Physiology, Cooperative Research Group, D–14476 Golm/Potsdam, Germany (M.M., S.B., M.-I.Z., B.M.-R.); and University of Potsdam, Institute of Biochemistry and Biology, D–14476 Golm/Potsdam, Germany (S.B., B.M.-R.)

We report about *ERF BUD ENHANCER* (*EBE*; At5g61890), a transcription factor that affects cell proliferation as well as axillary bud outgrowth and shoot branching in Arabidopsis (*Arabidopsis thaliana*). *EBE* encodes a member of the APETALA2/ETHYLENE RESPONSE FACTOR (AP2/ERF) transcription factor superfamily; the gene is strongly expressed in proliferating cells and is rapidly and transiently up-regulated in axillary meristems upon main stem decapitation. Overexpression of *EBE* promotes cell proliferation in growing calli, while the opposite is observed in *EBE-RNAi* lines. *EBE* overexpression also stimulates axillary bud formation and outgrowth, while repressing it results in inhibition of bud growth. Global transcriptome analysis of estradiol-inducible *EBE* overexpression lines revealed 48 EBE early-responsive genes, of which 14 were up-regulated and 34 were down-regulated. EBE activates several genes involved in cell cycle regulation and dormancy breaking, including D-type cyclin *CYCD3;3*, transcription regulator *DPa*, and *BRCA1-ASSOCIATED RING DOMAIN1*. Among the down-regulated genes were *DORMANCY-ASSOCIATED PROTEIN1* (*AtDRM1*), *AtDRM1 homolog*, *MEDIATOR OF ABA-REGULATED DORMANCY1*, and *ZINC FINGER HOMEODOMAIN5*. Our data indicate that the effect of EBE on shoot branching likely results from an activation of genes involved in cell cycle regulation and dormancy breaking.

The aerial shoot system and in particular the branching habit are central elements of the three-dimensional plant structure (Sussex and Kerk, 2001; McSteen and Leyser, 2005). Branch patterns vary widely within and between species; they contribute to the diversity of plant life forms and their ability to populate different ecological niches (Bonser and Aarssen, 2003). Plant architecture and, hence, the branching pattern is also an important attribute to modern crop species; changing the branching habit can help to optimize the use of resources for enhanced growth, biomass accumulation, and seed or fruit yield (García del Moral and García del Moral, 1995; Zhao et al., 2006; Doust, 2007; Boe and Beck, 2008).

The branching habit shows remarkable developmental plasticity controlled by an intricate interplay of various hormones, including auxin, strigolactone, and cytokinin (Wang and Li, 2006, 2008; Beveridge and Kyozuka, 2010; Domagalska and Leyser, 2011), and is also affected by many environmental factors, including light, temperature, humidity, and nutrient availability (Reinhardt and Kuhlemeier, 2002). Axillary shoot development begins with the initiation of an axillary meristem in the axil of a leaf to form a bud through subsequent cell proliferation. Depending on internal and environmental signals, the bud may then grow out farther to form an axillary shoot or (transiently) stop further cell division and remain in a dormant state before cell proliferation may resume later (Shimizu-Sato and Mori, 2001; Kebrom et al., 2006). Thus, molecular mechanisms coordinating progression through the cell cycle are expected to be of great relevance for bud formation and outgrowth (Horvath et al., 2003; Tatematsu et al., 2005).

Various experimental approaches have been used to study the regulation of axillary shoot development. Classical decapitation studies and application of phytohormones showed that auxin plays a central role in controlling shoot branching. Recent findings demonstrate that auxin moving down the plant not only promotes the production of strigolactone by stimulating the expression of strigolactone biosynthesis genes (Foo et al., 2005; Hayward et al., 2009) but also negatively regulates cytokinin content and import (to the bud) to suppress bud outgrowth (second messenger model; Li et al., 1995; Tanaka et al., 2006). Moreover, auxin export from the bud appears to be critical for its outgrowth (auxin transport canalization model; Domagalska and Leyser, 2011). Nevertheless, recent studies have proposed the existence of a rapid, indole acetic acid-independent signal acting as the trigger for

[1] Present address: Instituto de Biología Molecular y Celular de Rosario, Suipacha 570, S2002LRK Rosario, Argentina.

* Corresponding author; e-mail bmr@uni-potsdam.de.

The author responsible for distribution of materials integral to the findings presented in this article in accordance with the policy described in the Instructions for Authors (www.plantphysiol.org) is: Bernd Mueller-Roeber (bmr@uni-potsdam.de).

[W] The online version of this article contains Web-only data.

www.plantphysiol.org/cgi/doi/10.1104/pp.113.214049

bud outgrowth after decapitation. The signal might be a physical response to a change in turgor pressure or an electrical potential, rather than a chemical compound (Ferguson and Beveridge, 2009; Renton et al., 2012).

Although much has been learned about the hormonal control of shoot branching, little is currently known about regulatory processes acting in the bud itself. One of the most prominent bud-specific regulators is *TEOSINTE BRANCHED1* (*TB1*) from maize (*Zea mays*; Doebley et al., 1997), a member of the plant-specific TCP (for TB1, CYCLOIDEA, and PCF domain) family of transcription factors (Martín-Trillo and Cubas, 2010); similarly, *TB1* homologs from other species, including *BRANCHED1* (*BRC1* [At3g18550]; also called *TEOSINTE BRANCHED1-LIKE1* [*TBL1*] or TCP18; Aguilar-Martínez et al., 2007; Finlayson, 2007) and *BRC2* (*TCP12*) in Arabidopsis (*Arabidopsis thaliana*) and *SlBRC1b* in tomato (*Solanum lycopersicum*; Martín-Trillo et al., 2011; for review, see Domagalska and Leyser, 2011), control shoot branching. Generally, expression of these genes is largely restricted to axillary meristems and buds, and loss of functional *TB1*, *BRC1*, or *BRC2* genes leads to increased branching, while overexpressing *TB1* homologs inhibits branching (Aguilar-Martínez et al., 2007; Finlayson, 2007; Martín-Trillo et al., 2011).

Most cells in dormant axillary buds are arrested at the G1 phase of the cell cycle (Devitt and Stafstrom, 1995; Shimizu and Mori, 1998), and experimental evidence suggests that TCP transcription factors regulate the transition from the G1 to the S phase (Kosugi and Ohashi, 1997). In dormant axillary buds of pea (*Pisum sativum*), transcript levels of various cell cycle-related genes, such as *PROLIFERATING CELL NUCLEAR ANTIGEN*, *CYCB1;2* (B-type cyclin), *CYCD3;1* (D-type cyclin), and *CELL DIVISION CYCLE2*, were very low, but expression of all genes increased after decapitation in a cell cycle-dependent fashion (Shimizu and Mori, 1998; Shimizu-Sato and Mori, 2001). Global expression profiling confirmed the up-regulation of many cell cycle-related genes in axillary shoots upon main stem decapitation, in addition to genes encoding ribosomal proteins (Tatematsu et al., 2005). In addition, other genes, often of vaguely defined molecular or biochemical functions, are affected in axillary buds by main stem decapitation. In Arabidopsis, expression of the dormancy-associated genes *AtDRM1* (At1g28330) and *AtDRM1 homolog* (At2g33830) is strongly down-regulated within the first 12 to 24 h after main shoot decapitation, while expression of both genes increases again thereafter (Tatematsu et al., 2005). Similarly, expression of the *DRM1* ortholog from pea (*PsDRM1*) strongly declines within several hours of decapitation, while it rapidly resumes when buds become dormant again, revealing it as a good dormancy marker (Stafstrom et al., 1998).

Here, we report about *ERF BUD ENHANCER* (*EBE*; At5g61890), a new transcriptional regulator of -cell proliferation and axillary bud outgrowth in Arabidopsis. EBE is a member of the APETALA2/ETHYLENE RESPONSE FACTOR (AP2/ERF) transcription factor superfamily that encompasses 147 members in Arabidopsis (Nakano et al., 2006). The *EBE* gene is strongly expressed in proliferating cells, with preferential expression during the S phase of the cell cycle. Overexpression of *EBE* promotes cell proliferation, leading to enhanced callus growth, while the opposite is observed in *EBE-RNAi* lines. In addition, *EBE* overexpression in transgenic plants stimulates axillary bud formation and outgrowth, while its repression inhibits bud growth. The effect of EBE on shoot branching likely results from affecting genes involved in cell cycle regulation and dormancy breaking.

RESULTS

EBE Is Prominently Expressed in Proliferating Cells

To discover transcription factors controlling vegetative development, we screened transgenic Arabidopsis lines ectopically expressing transcription factors under the control of the cauliflower mosaic virus (CaMV) 35S promoter. One of the lines that attracted our attention overexpressed an uncharacterized AP2/ERF transcription factor encoded by gene locus *At5g61890*. As we show below, *At5g61890* promotes axillary bud growth; therefore, we named it *EBE*. EBE belongs to group Xa of the ERF family of the AP2/ERF superfamily; group Xa includes six genes in Arabidopsis and seven genes in rice (*Oryza sativa*; Nakano et al., 2006). Like other members of ERF group Xa, EBE harbors a characteristic CMX-1 motif of unknown function in its N-terminal region.

By analyzing public transcriptome data (Genevestigator; Zimmermann et al., 2004), we found that expression of *EBE* is particularly strong in undifferentiated cells of suspension cultures and in calli. In a global transcriptome data set of Menges et al. (2003), we observed preferential *EBE* expression during the S phase of the cell cycle, whereas expression was low in other phases (Fig. 1A). To test whether *EBE* expression in proliferating cells is controlled at the promoter level, we fused its approximately 2-kb promoter to the *GUS* reporter gene and tested GUS activity in transgenic $Prom_{EBE}$:*GUS* Arabidopsis plants. Cotyledon segments of three independent $Prom_{EBE}$:*GUS* lines were incubated on callus-induction medium (CIM). Strong GUS activity was observed in callus (Fig. 1B), while GUS activity was weaker in regenerating shoots (Fig. 1C), and no GUS activity was detected in young regenerating roots. Similarly, in a global transcriptome analysis using Affymetrix ATH1 microarrays, *EBE* was up-regulated during callus formation 4 and 7 d after incubation in CIM (Che et al., 2006), and it was approximately 3.5-fold up-regulated in *Agrobacterium tumefaciens*-induced Arabidopsis tumors when compared with tumor-free inflorescence stalk tissue (Deeken et al., 2006). Rapid cell proliferation in tumors is stimulated by high concentrations of cytokinin and auxin synthesized by transfer

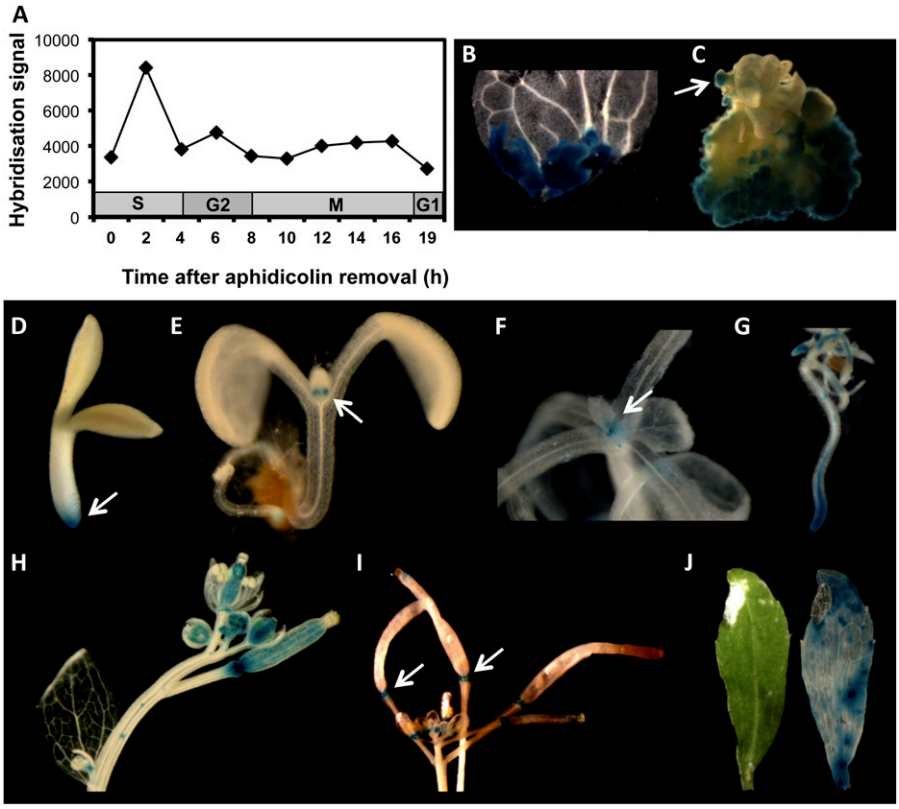

Figure 1. *EBE* expression. A, *EBE* expression during cell cycle progression. Data were extracted from Menges et al. (2003), using Genevestigator. B to J, *EBE* promoter-driven GUS activity. B and C, GUS activity in calli and regenerating shoot (arrow in C). D and E, Three- and 9-d-old seedlings, respectively. Note GUS staining in the root tip and stipules (arrows). F, Shoot, with staining at the apex (arrow). G, Roots. H, Flowers and young siliques. I, Old siliques, with GUS staining in abscission zones (arrows). J, Senescent leaf: left, unstained; right, GUS stained. Incubation in GUS staining solution was done overnight.

DNA (T-DNA)-encoded bacterial enzymes. Indeed, tumor growth in plants is reminiscent of callus formation in CIM, supporting our above results. Similarly, *EBE* expression increased by approximately 10-fold in regenerating stumps of root tips within 5 h after removal of the tip (Sena et al., 2009), and it increased to a similar extent in callus derived from cotyledons and petals (Sugimoto et al., 2010). Using $Prom_{EBE}$:*GUS* plants, we observed strong GUS staining several hours after wounding of leaves, when callus formation resumed at wound sites (data not shown). Collectively, these data demonstrate that *EBE* expression is particularly prominent in proliferating cells.

We also analyzed the expression pattern of *EBE* in whole plants. In 3- to 8-d-old seedlings, GUS activity was detected in root tips (Fig. 1D), stipules (Fig. 1E), and the shoot apex (Fig. 1F). Prominent *EBE* expression was also observed in tips of lateral roots (Fig. 1G) and various floral tissues (Fig. 1H). Comparatively, strong *EBE* expression was observed in young siliques (Fig. 1H), while expression in old siliques was largely restricted to abscission zones (Fig. 1I). Weak *EBE* expression was normally observed during early leaf development, whereas it was virtually absent in bigger leaves but resumed upon leaf senescence (Fig. 1J). We also measured *EBE* transcript abundance by quantitative reverse transcription (qRT)-PCR in immature and partially (approximately 20%) senescent leaves and found approximately 10-fold higher expression in the latter (data not shown). In some plant lines, hypocotyls and a small area of the cotyledon tip and petioles also showed $Prom_{EBE}$-driven GUS activity.

EBE Overexpression Promotes Callus Growth and Triggers Neoplastic Activity

To assess the in vivo function of *EBE*, we generated *35S*:*EBE* overexpression lines and chose three representative lines (#11, #21, and #28) for detailed studies. Additionally, we inhibited *EBE* expression by RNA interference (RNAi) and selected lines (including *EBE-RNAi* #10, #22 and #17) with strongly reduced *EBE* transcript abundance in rosette leaves (see below) for analysis.

The prominent expression of *EBE* in proliferating cells and calli prompted us to analyze the effect of *EBE* overexpression and inhibition on callus formation and shoot and root development. First, cotyledon or young leaf segments obtained from the transgenic *35S*:*EBE* and *EBE-RNAi* lines as well as from Arabidopsis ecotype Columbia (Col-0) plants were precultured on CIM for 4 d and then transferred to shoot-induction medium, root-induction medium, or fresh CIM for 4 weeks. The sizes and number of the calli formed, the number of adventitious shoots, and root formation were analyzed weekly. With respect to the capacities for shoot or root regeneration, we did not detect significant differences between *35S*:*EBE*, *EBE-RNAi*, and wild-type plants. However, calli formed from the *35S*:

EBE lines were considerably larger than those of the wild type, and *EBE-RNAi* calli were smaller (Fig. 2, A and B). We analyzed cell sizes in *35S:EBE*, *EBE-RNAi*, and wild-type calli and observed smaller cells in *EBE* overexpressors than in RNAi lines (Fig. 2C); thus, larger calli observed in *EBE* overexpressors appear to result from more pronounced cell proliferation leading to an increased cell number.

A prominent feature observed in *35S:EBE* plants was neoplasia; tissue similar to green callus often produced "organ-like" structures at wounded sites (or partially senesced tissue) in the absence of external phytohormones (Supplemental Fig. S1, A–C). Upon extended growth, such calli regularly differentiated into organs such as roots, leaves, or shoots (data not shown), while neoplasia was very rarely observed in wild-type plants kept under identical conditions. Cell proliferation and callus formation can be induced from differentiated plant tissues by phytohormone treatment (Mizukami and Fischer, 2000). Apparently, ectopic overexpression of *EBE* reduces the dependence on external hormones for reentry into the cell cycle and cell proliferation.

EBE Affects Shoot Branching

35S:EBE plants remained smaller and produced more first-order lateral rosette branches than the parent wild type (Fig. 3, A and B). After 28 d of growth, wild-type plants displayed around six lateral branches while *35S:EBE* lines #21, #11, and #28 displayed about nine, 15, and 20 lateral branches, respectively (Supplemental Fig. S2A). qRT-PCR revealed low *EBE* expression in leaves of 4-week-old wild-type plants. In *35S:EBE* transgenic plants, *EBE* transcript abundance was positively correlated with the strength of the observed phenotype. *EBE* expression level determined by qRT-PCR was approximately 10 times lower in line *35S:EBE* #21, which displayed a weaker phenotype, than in the strong-phenotype lines #11 and #28 (Supplemental Fig. S2B).

We next analyzed an Arabidopsis mutant (*ebe-1D*; SALK_000833) carrying a T-DNA insertion approximately 400 bp upstream of the *EBE* translation initiation codon (ATG). Homozygous *ebe-1D* insertion lines, identified by PCR on genomic DNA (Supplemental Fig. S3A), phenotypically resembled *35S:EBE* lines (first-order lateral branches were more abundant than in the wild type; Fig. 3, A and B; Supplemental Fig. S3, B and C). In contrast, heterozygous T-DNA insertion lines showed normal growth indistinguishable from the wild type (data not shown). Segregation analysis indicated that *ebe-1D* had a single T-DNA insertion (data not shown). Expression analysis by qRT-PCR revealed approximately 6-fold elevated *EBE* transcript abundance in the homozygous *ebe-1D* mutant compared with the wild type, while *EBE* expression level was enhanced by up to approximately 10-fold in the *35S:EBE-21* line (Supplemental Fig. S3D). Thus, as in *35S:EBE* lines, elevated *EBE* expression coincided with enhanced formation of lateral branches.

In approximately 4-week-old RNAi lines #10, #22, and #17, *EBE* transcript level was approximately six, 15, and 27 times, respectively, lower than in Col-0 wild-type plants (Supplemental Fig. S4A). All RNAi lines produced fewer first-order rosette lateral branches than Col-0, and the inhibition level of *EBE* expression followed the strength of the observed phenotype (Supplemental Fig. S4B). However, the number of first-order (and second-order) cauline branches did not change in *EBE* transgenic plants compared with the wild type (Supplemental Table S1). Final plant height was reduced in *35S:EBE* lines compared with the wild type; a similar observation was made for *ebe-1D*

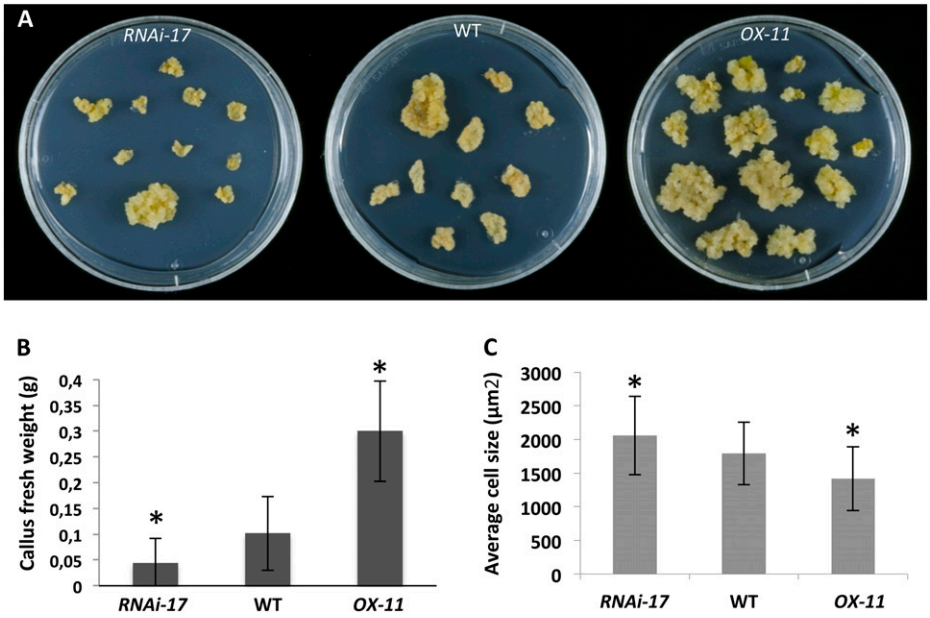

Figure 2. Effects of altered *EBE* expression on callus formation. A and B, Overexpression of *EBE* increases callus size. Data in B represent mean fresh weight ± SD of at least 30 calli, grown in three independent biological experiments. C, Size of cells in calli. Data are means of at least 120 cells each ± SD. In B, asterisks indicate statistically significant differences between the wild type (WT) and either *EBE-RNAi-17* or *35S:EBE* (*OX-11*) calli (Student's *t* test after false discovery rate correction, $P < 0.01$). In C, asterisks indicate statistically significant differences between *EBE-RNAi-17* and *35S:EBE* (*OX-11*) calli (Student's *t* test, $P < 0.05$).

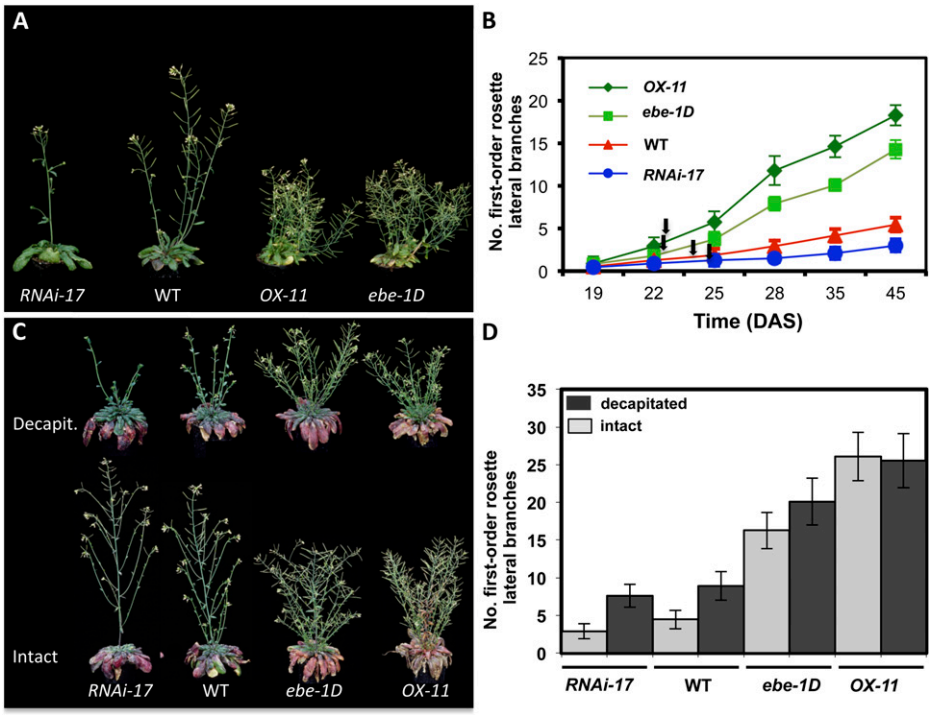

Figure 3. Phenotypic effects of altered *EBE* transcript level. A, Phenotypes of 33-d-old transgenic *EBE* lines compared with wild-type (WT) plants, grown in long-day conditions. B, Number of first-order rosette lateral branches in *35S:EBE* (*OX-11*), *ebe-1D*, wild-type, and *EBE-RNAi-17* plants. Given are means ± SD of 11 different plants of each line at each stage. At time points 28, 35, and 45 d after sowing (DAS), the differences between wild-type and all transgenic plants are statistically significant (Student's *t* test after false discovery rate correction, $P < 0.01$). Arrows indicate flowering time for each line. Flowering time of the transgenic plants did not significantly differ from that of the wild type under our experimental conditions (Student's *t* test after false discovery rate correction, $P > 0.05$; Supplemental Table S5). C, Phenotype of transgenic plants 12 d after decapitation (top) compared with intact plants that were not decapitated (bottom). Plants were 3 months old. D, Number of first-order rosette lateral branches of wild-type and transgenic plants at 12 d after removal of the main shoot, compared with intact plants. In wild-type plants, approximately 50% of the buds in primary rosette branches grew out, whereas in *RNAi*, *ebe-1D*, and *OX-11* lines, approximately 38%, 80%, and 100%, respectively, of the buds did. Data represent means ± SD ($n = 11$). Data for intact versus decapitated plants were significantly different for all lines except the strong *EBE* overexpressor line *OX-11* (Student's *t* test, $P < 0.01$).

(Supplemental Table S2), consistent with its elevated *EBE* expression.

EBE Promotes Axillary Bud Formation and Outgrowth

A well-known developmental phenomenon in plants is apical dominance controlled by the main shoot apical meristem (SAM). Upon decapitation, the inhibitory effect of auxin on axillary buds is removed, resulting in cell proliferation and bud outgrowth. To examine whether the altered number of axillary (i.e. first-order rosette lateral) branches in transgenic plants results from a general effect on lateral bud outgrowth, axillary shoot formation was analyzed in wild-type and transgenic plants before and after main shoot decapitation. In intact (i.e. nondecapitated) plants, the number of axillary shoots was approximately three, five, 16, and 26 in *EBE-RNAi-17*, the wild type, *ebe-1D*, and *35S:EBE #11*, respectively (Fig. 3, C and D), following the level of *EBE* expression. To test the effect of decapitation, plants were first grown under short-day conditions for 30 d and then shifted to long-day conditions to induce flowering. Primary shoots were removed at a size of approximately 10 cm. Twelve days after decapitation, wild-type plants had developed approximately nine axillary shoots, whereas *EBE-RNAi-17*, *ebe-1D*, and *35S:EBE #11* had produced approximately seven, 20, and 25 axillary shoots, respectively (Fig. 3, C and D). Thus, while additional axillary shoots were formed in wild-type and RNAi plants (about twice as many under decapitation than intact conditions), no additional axillary shoots formed upon decapitation in plants overexpressing *EBE* (which already had many more axillary shoots in intact plants). The stimulatory effect of decapitation on axillary shoot formation was slightly more pronounced in the RNAi line than in the wild type, indicating that the RNAi-mediated inhibitory effect is partly overcome when expression of the endogenous *EBE* gene is induced by decapitation (see below). In nondecapitated wild-type plants, more axillary

shoots are produced than in RNAi lines, reflecting the higher basal ("decapitation-independent") level of *EBE* expression in the wild type. The decapitation-induced effect on axillary shoot formation is then less pronounced in the wild type than in RNAi lines.

To further substantiate the conclusion that *EBE* affects axillary bud formation, we analyzed the presence of vegetative buds in wild-type and transgenic plants. In accordance with published reports (Grbic, 2005), wild-type plants did not form buds in their cotyledonary nodes. Similarly, buds were absent in cotyledonary nodes of RNAi lines. In contrast, both *35S:EBE* and *ebe-1D* lines produced cotyledonary buds (data not shown).

Four weeks after sowing, wild-type and transgenic plants grown under long-day conditions had started flowering, and axillary meristems were initiated in a basipetal order. In wild-type plants, buds closest to the shoot apex were developmentally more advanced than more distant ones; cotyledons and most of the L1 and L2 leaves (which developed after the cotyledons) had no axillary buds, while leaves L3 to L9 generally had buds in vegetative stage 1 or 2 (i.e. did not yet have flowers). One-half of the L10 to L12 leaves contained flowering buds in their axils (Fig. 4A). In contrast, in *EBE-RNAi* lines, only a few L10, L11, and L12 leaves had flowering buds (Fig. 4B), while in *35S:EBE* and *ebe-1D* plants, flowering buds developed in a high percentage of young leaves (Fig. 4, C and D).

In conclusion, our data indicate that *EBE* influences cellular processes, most likely by affecting cell cycle progression and cell proliferation, during axillary shoot formation in both intact and decapitated plants.

Main Stem Decapitation Stimulates *EBE* Expression in Axillary Buds

As main stem decapitation promotes axillary bud outgrowth, we tested decapitation-dependent expression of *EBE* in the $Prom_{EBE}$:*GUS* lines. Main stems (2–5 cm long) were decapitated when axillary buds were visible. Low *EBE* promoter-dependent GUS activity was visible in axillary nodes of intact plants, but this activity remarkably increased 6 h after decapitation (Fig. 5, A and B). Decapitation-controlled expression of *EBE* was confirmed by qRT-PCR in wild-type Arabidopsis plants. *EBE* transcript abundance was measured in the five uppermost axillary branches developing from either decapitated or intact main stems (control). *EBE* expression level increased transiently (by up to approximately 3-fold) 6 to 15 h after decapitation of the main stem (Fig. 5C). As a control, we included *AtDRM1* (At1g28330), the transcript abundance of which decreased upon decapitation (Fig. 5D), as reported (Tatematsu et al., 2005; Aguilar-Martínez et al., 2007).

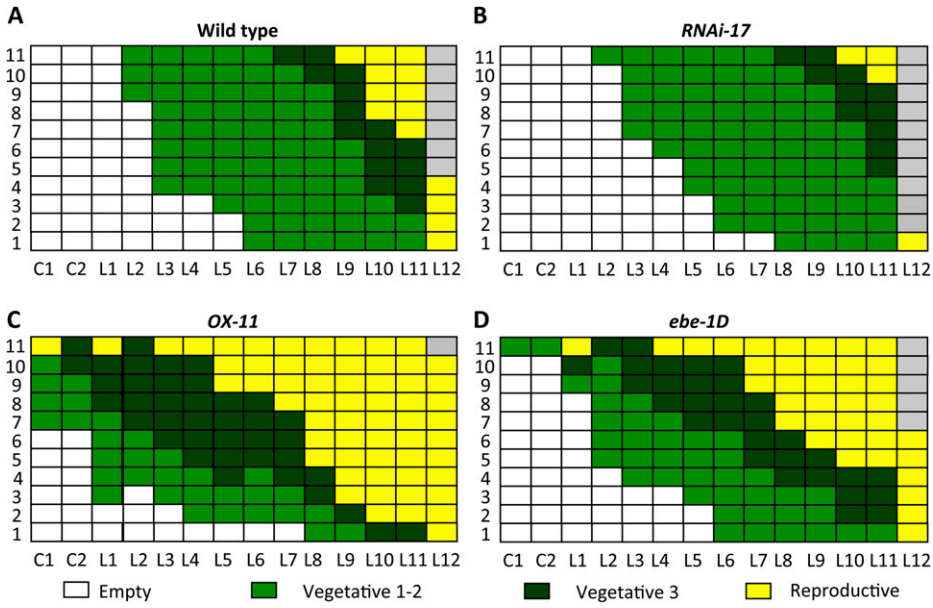

Figure 4. Developmental stages of buds in the axils of cotyledons (C1 and C2) and rosette leaves (L1–L12) shown on the *x* axis. The experiment was performed with 11 4-week-old plants grown under long-day conditions, indicated by numbers on the *y* axis. As *EBE-RNAi-17* lines had developed approximately 12 leaves at the analysis time point, data of 12 rosette leaves (L1–L12) are presented for all lines. A, The wild type. B, *EBE-RNAi-17*. C, *35S:EBE* (*OX-11*). D, *ebe-1D*. The bud developmental gradient was found to be more pronounced in *EBE-RNAi* lines than in the wild type but to be less obvious in *35S:EBE* and *ebe-1D* lines. Developmental stages are as follows: vegetative 1, buds with two or more leaf primordia formed, no trichomes, 150 to 250 μm; vegetative 2, mid vegetative stage, buds with differentiating trichome-bearing leaf primordia, less than 400 μm; vegetative 3, late vegetative stage, buds with expanding trichome-bearing leaf primordia, more than 400 μm; reproductive, flower meristems visible within the bud.

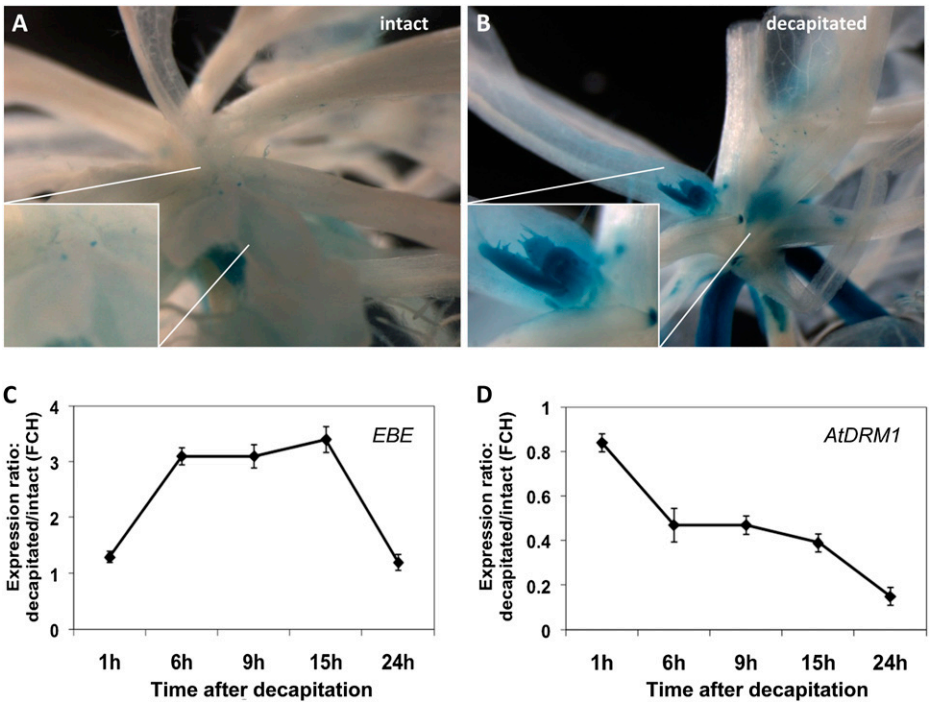

Figure 5. Altered *EBE* expression before and after decapitation. A and B, GUS staining of axillary shoots before (A) and 6 h after (B) main stem decapitation. C and D, qRT-PCR analysis of *EBE* (C) and *AtDRM1* (D) expression in the five uppermost axillary shoots after main stem decapitation. Symbols in both panels represent means ± SD of three biological experiments. FCH, Fold change.

EBE Contributes to the Maintenance of the SAM and Affects Plastochron

One week after germination, when grown in short-day conditions, we did not observe macroscopic differences between transgenic and wild-type plants, while at 2 weeks, a change in the leaf plastochron (the time interval between the initiation of successive leaves) was evident: leaf initiation occurred in shorter time intervals in *35S:EBE* and *ebe-1D* plants compared with the wild type, reminiscent of a shorter plastochron, whereas plastochron was longer in *EBE-RNAi* lines (Fig. 6, A and B). Additionally, leaf size remained generally smaller in *35S:EBE* #28 and *ebe-1D*, while it was increased in *EBE-RNAi* plants compared with the wild type (Fig. 3A; Supplemental Fig. S5A). In accordance with this observation, cell sizes were smaller in *35S:EBE* than in wild-type plants (similar to cells in calli, as reported above) and bigger in RNAi plants (Supplemental Fig. S5, B and C).

It is well established in Arabidopsis that cotyledons and the first pair of true leaves emerge in an approximately decussate (180°) arrangement (Mündermann et al., 2005). We observed that phyllotaxy of the first pair of true leaves was altered in plants strongly overexpressing *EBE* (Fig. 6C): of 38 *35S:EBE-21* plants analyzed, the majority (22 plants) had an angle of 120° to 160°, five plants showed an angle of about 100° to 120°, and 11 plants showed an angle close to 180°C. In contrast, of 55 wild-type plants analyzed, only four displayed an angle of less than 180°. Similarly, of 19 *ebe-1D* plants tested, the majority displayed an angle of 180°, and five showed an angle between 120° and 160°. Thirty-six of 43 *EBE-RNAi-17* plants tested had a normal angle of approximately 180°, and seven lines showed an angle of 140° to 160°.

In addition, in some cases, the size of the SAM was abnormally enlarged in *35S:EBE* plants (Fig. 6C), so that SAM development arrested after the formation of a few leaves. Development also arrested in some *EBE-RNAi* lines after cotyledon growth (Fig. 6C). Analysis by scanning electron microscopy revealed that in some *35S:EBE* plants, a leaf primordium was initiated but then moved away from the meristem without developing further (Supplemental Fig. S6A). Such abortive leaf primordia were never observed in wild-type plants under our experimental conditions.

We also analyzed GUS staining in the shoot apex of $Prom_{EBE}$:*GUS* plants. We observed low but still detectable GUS activity in early leaf primordia (Supplemental Fig. S6B). Taken together, these results suggest a likely involvement of *EBE* in maintaining the structure of the SAM as well as plastochron and phyllotaxy.

EBE-Triggered Changes in Gene Expression

To identify genes downstream of EBE, we generated transgenic Arabidopsis lines expressing *EBE* under the control of an estradiol-inducible promoter (*EBE-XVE* lines) using the system of Zuo et al. (2000). Transgenic seedlings precultured on agar-solidified Murashige and Skoog (MS) medium were transferred to liquid MS medium supplemented with 2 μM β-estradiol (EST). Wild-type control plants (Col-0) were treated in the same way. Leaves of the EST-treated plants were harvested after different time points (from 30 min to 20

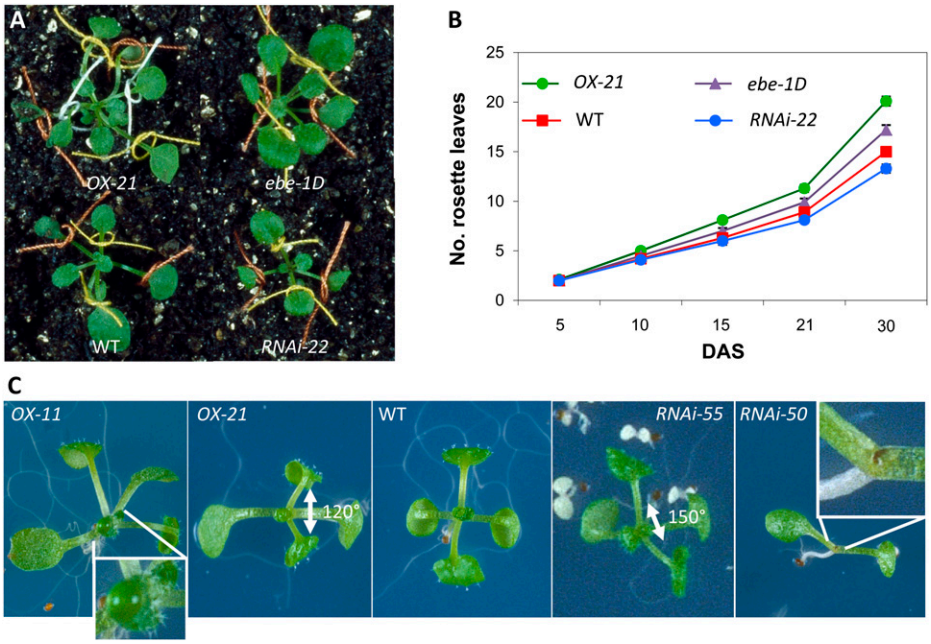

Figure 6. Effects of altered *EBE* expression on plant phenotype. A, *EBE* up-regulation causes an increase and its down-regulation causes a decrease of the leaf initiation rate as compared with the wild type (WT). Threads of the following colors were used for labeling rosette leaves: orange for leaves L1 and L2, yellow for leaves L3 and L4, and white for leaves L5 and L6. B, Number of rosette leaves of transgenic and wild-type plants during a period of 4 weeks. The symbols represent means ± SD of 11 plants at each time point. At 30 d after sowing (DAS), there is a statistically significant difference between the wild type and all transgenic plants (Student's *t* test after false discovery rate correction, $P < 0.05$). C, Altered phyllotaxy and SAM size in transgenic plants compared with the wild type. The left panel shows an enlarged SAM in a *35S:EBE* plant (*OX-11*) that had arrested without developing further. The right panel shows an arrested SAM in the *EBE-RNAi-50* line that occurred after cotyledon development. The three middle panels show the changed phyllotaxy of transgenic plants in comparison with the wild type. In some of the *35S:EBE* plants, the angle between the two first true leaves was only about 120°, while in *EBE-RNAi* plants, the angle was more than 150°C.

h) and tested for *EBE* expression by qRT-PCR; enhanced *EBE* expression was already detected at the earliest time point. From four different lines analyzed, we selected *EBE-XVE* #14 (*XVE-14*) for further experiments (Supplemental Fig. S7A). To test the effect of chemically induced *EBE* overexpression on early seedling development, we cultured *XVE-14* (and Col-0) seedlings for 4 d on MS agar plates and then transferred them to liquid MS medium containing 10 μM EST. As seen in Supplemental Figure S7B, *XVE-14* seedlings developed primary leaves more rapidly than wild-type seedlings and produced more lateral roots, further supporting a role of *EBE* in plant development.

To identify genes affected by EBE, we studied the transcriptomes in shoots of *XVE-14* and wild-type seedlings after 45 min of EST (2 μM) treatment using Affymetrix ATH1 arrays (three biological replications each). Genes showing an expression change of greater than 1.5-fold in all three experiments in *XVE-14* but not in wild-type plants were considered to be downstream of EBE. We identified nine up-regulated and 26 down-regulated genes in the *EBE*-inducible line. Expression of some additional genes was significantly altered in two of the three experiments. We tested the expression of these genes in EST-induced *XVE-14* and wild-type plants by qRT-PCR (three biological replicates), confirming differential expression of an additional five up-regulated and eight down-regulated genes. Table I lists all 48 genes robustly affected by inducible *EBE* overexpression.

Notably, of the 14 genes rapidly up-regulated by EBE, three were cell cycle related, including D-type cyclin *CYCD3;3* (At3g50070; 2.8-fold), transcription regulator *DPa* (At5g02470; 2.4-fold), and *BRCA1-ASSOCIATED RING DOMAIN1* (*BARD1*; At1g04020; 2.5-fold). *CYCD3;3* transcripts accumulate in the early G1 phase during cell cycle reentry (Menges et al., 2005), and dormancy breaking is generally accompanied by increased expression of *CYCD* genes (Horvath et al., 2003). *DPa*, along with *E2Fa*, is expressed in actively dividing tissues of the SAM, young leaf primordia, vascular tissues of maturing leaf primordia, and axillary buds. DPa interacts with the E2Fa transcription factor to form a complex that stimulates the expression of S phase-specific genes, leading to cell division and a delay of cell differentiation (De Veylder et al., 2002). *BARD1* has been reported to control SAM organization and maintenance by restricting *WUSCHEL* (*WUS*) expression to the organizing center (Han et al., 2008). *WUS* encodes a homeodomain

Table I. *List of genes differentially expressed in EST-inducible EBE overexpression line 14 compared with wild-type plants at 45 min after EST induction*

Three independent biological replications were performed. Numbers represent the expression ratio (fold change). Average values and SD are given as well. Genes are ordered according to their fold change. Asterisks are as follows: *transcription factors up-regulated by EBE; **transcription factors down-regulated by EBE. Bio1, Bio2, and Bio3 represent the first, second, and third biological replicates, respectively.

Affy Identifier	Arabidopsis Genome Initiative Identifier	Annotation	Bio1	Bio2	Bio3	Average	SD
266743_at	At2g02990[a]	RNS1 (RNase1)	9.46	13.1	5.45	9.34	3.83
257673_at	At3g20370	TRAF-like family protein	2.78	13.3	2.10	6.07	6.29
266294_at	At2g29500[a]	HSP20-like chaperone superfamily protein	5.74	3.66	3.48	4.29	1.25
252189_at	At3g50070[a]	CYCD3;3 (cyclin D3;3)	3.02	2.50	2.80	2.77	0.26
262680_at	At1g75880	SGNH hydrolase-type esterase superfamily protein	3.01	2.99	2.30	2.77	0.41
259173_at	At3g03640	BGLU25 (β-glucosidase25)	1.65	4.73	1.55	2.64	1.81
265097_at	at1g04020[a]	ATBARD1 (BRCA1-associated RING domain1)	2.83	1.94	2.76	2.51	0.49
251052_at	At5g02470[a]	DPa; transcription factor*	2.97	2.65	1.68	2.43	0.67
251181_at	At3g62820	Invertase/pectin methylesterase inhibitor family protein	1.75	1.99	2.20	1.98	0.23
264782_at	At1g08810	AtMYB60; transcription factor*	2.54	1.86	1.54	1.98	0.51
267628_at	At2g42280	bHLH130; transcription factor*	1.72	1.70	2.10	1.84	0.23
249112_at	At5g43780	APS4	1.57	1.81	1.96	1.78	0.20
267305_at	At2g30070	ATKT1-ATKUP1 (K^+ uptake1)	1.74	1.59	1.57	1.64	0.09
251556_at	At3g58840	Tropomyosin related	1.52	1.75	1.55	1.61	0.13
267092_at	At2g38120[a]	AUX1 (auxin resistant1)	0.53	0.59	0.61	0.58	0.04
255433_at	At4g03210	AtXTH9	0.54	0.61	0.57	0.57	0.04
246996_at	At5g67420[a]	LBD37; transcription factor**	0.65	0.57	0.50	0.57	0.08
246002_at	At5g20740	Invertase/pectin methylesterase inhibitor family protein	0.6	0.63	0.47	0.57	0.08
266391_at	At2g41290	Strictosidine synthase like	0.53	0.50	0.61	0.55	0.06
261375_at	At1g53160[a]	SPL4; transcription factor**	0.65	0.44	0.56	0.55	0.10
253608_at	At4g30290	AtXTH19	0.64	0.52	0.47	0.54	0.09
260560_at	At2g43590	Chitinase, putative	0.60	0.45	0.55	0.53	0.08
246906_at	At5g25475	AP2/B3-like transcription factor**	0.60	0.43	0.56	0.53	0.09
253815_at	At4g28250[a]	ATEXPB3 (expansin B3)	0.62	0.31	0.64	0.52	0.19
255872_at	At2g30360	CIPK11	0.52	0.39	0.62	0.51	0.11
256452_at	At1g75240	AtHB33; transcription factor**	0.58	0.43	0.46	0.49	0.08
262986_at	At1g23390	Kelch repeat-containing F-box family protein	0.60	0.24	0.63	0.49	0.22
263951_at	At2g35960	NHL12 (NDR1/HIN1-like12)	0.55	0.36	0.55	0.48	0.11
266300_at	At2g01420[a]	PIN4 (pin-formed4)	0.37	0.4	0.63	0.47	0.14
252063_at	At3g51590	LTP12 (lipid transfer protein12)	0.30	0.5	0.57	0.46	0.14
267460_at	At2g33810	SPL3; transcription factor**	0.60	0.31	0.46	0.46	0.15
252549_at	At3g45860	CRK4; Cys-rich RLK	0.34	0.37	0.66	0.46	0.18
266223_at	At2g28790	Thaumatin superfamily protein	0.64	0.29	0.35	0.43	0.19
245265_at	At4g14400	ACD6 (accelerated cell death6)	0.57	0.09	0.56	0.41	0.27
248062_at	At5g55450	Protease inhibitor/seed storage/lipid transfer protein family protein	0.30	0.38	0.48	0.39	0.09
245668_at	At1g28330[a]	AtDRM1 (dormancy-associated protein1)	0.41	0.10	0.55	0.35	0.23
247718_at	At5g59310	LTP4 (lipid transfer protein4)	0.20	0.42	0.41	0.34	0.12
251169_at	At3g63210[a]	MARD1 (mediator of abscisic acid-regulated dormancy1)	0.30	0.27	0.40	0.32	0.07
253061_at	At4g37610	BT5 (BTB and TAZ domain protein5); transcription regulator**	0.24	0.44	0.23	0.30	0.12
252269_at	At3g49580	LSU1; response to low sulfur1	0.35	0.27	0.27	0.29	0.05
260038_at	At1g68875	Unknown protein	0.38	0.26	0.17	0.27	0.10
265117_at	At1g62500	Protease inhibitor/seed storage/lipid transfer protein family protein	0.30	0.26	0.19	0.25	0.05
256597_at	At3g28500	60S acidic ribosomal protein P2	0.12	0.35	0.29	0.25	0.12
257421_at	At1g12030	Similar to unknown protein	0.19	0.14	0.44	0.25	0.16
267461_at	At2g33830[a]	AtDRM1 homolog	0.22	0.12	0.39	0.24	0.14
258675_at	At3g08770	LTP6 (lipid transfer protein6)	0.42	0.09	0.16	0.22	0.18
247717_at	At5g59320	LTP3 (lipid transfer protein3)	0.13	0.15	0.23	0.17	0.05
259802_at	At1g72260	THI2.1 (thionin2.1)	0.10	0.02	0.10	0.07	0.04

[a]Genes gained from qRT-PCR experiments; other genes were obtained from microarray analyses.

protein important for stem cell regeneration in the SAM (Mayer et al., 1998). Two further up-regulated genes encode the transcription factors bHLH130 (At2g42280) and AtMYB60 (At1g08810); however, their potential roles in shoot branching are not known.

AtDRM1 (At1g28330), *AtDRM1 homolog* (At2g33830), and *MEDIATOR OF ABA-REGULATED DORMANCY1* (*MARD1/SAG102*; At3g63210) were strongly down-regulated after *EBE* induction. Notably, *AtDRM1* and *AtDRM1 homolog* are also remarkably down-regulated

upon initiation of bud growth (Tatematsu et al., 2005), while *MARD1* has so far only been shown to affect seed dormancy control (He and Gan, 2004).

Several of the down-regulated genes encode lipid transfer proteins (AtLTP3, At5g59320; AtLTP4, At5g59310; AtLTP6, At3g08770; AtLTP12, At3g51590). LTPs are ubiquitous plant lipid-binding proteins proposed to function in various developmental and stress responses, signaling, and cell wall loosening (Kader, 1996; Bakan et al., 2006; Yeats and Rose, 2008). Furthermore, expression of the cell wall-loosening gene *AtEXPB3* (At4g28250; encoding expansin) and the xyloglucan endotransglucosylase/hydrolase genes *AtXTH9* (At4g03210) and *AtXTH19* (At4g30290) was markedly reduced upon *EBE* induction. Finally, a thaumatin-like protein (At2g28790) located in the cell wall (Bayer et al., 2006) and a putative chitinase (At2g43590) potentially involved in modulating cell expansion (Kwon et al., 2005) were also down-regulated. Collectively, EBE appears to exert part of its function by affecting the expression of genes encoding different types of cell wall-remodeling proteins.

AUX1 (At2g38120), which encodes an auxin influx carrier, was also down-regulated. During leaf initiation, AUX1 contributes to controlling a regular angle of 137.5° between successive primordia (Bainbridge et al., 2008).

Six of the 34 down-regulated genes encode transcription factors (Table I). ZINC-FINGER HOMEODOMAIN5 (ZHD5; At1g75240), also called ARABIDOPSIS THALIANA HOMEOBOX PROTEIN33, has recently been shown to stimulate shoot growth and the formation of larger leaves upon overexpression. Conversely, inhibition of ZHD5 at the protein level by overexpressing an interacting inhibitor peptide (mini zinc finger 1) resulted in dwarfish plants with small leaves (Hong et al., 2011). These phenotypes are consistent with growth phenotypes observed in our experiments, where overexpression of *EBE*, thereby lowering *ZHD5* expression, similarly caused dwarfish plants with small leaves and multiple shoots, and reducing *EBE* expression by RNAi inhibits axillary bud outgrowth and promotes the formation of larger leaves. *LATERAL ORGAN BOUNDARY DOMAIN37* (*LBD37*; At5g67420) is another down-regulated transcription factor that has been shown recently to affect nitrogen-dependent basal shoot branching, although its mode of action in this process has not been reported (Rubin et al., 2009). The transcriptional regulators SPL3 (At2g33810) and SPL4 (At1g53160) stimulate vegetative phase change and flowering and are suppressed by *miR156* (Wu and Poethig, 2006), but their role in bud outgrowth has not been studied in detail yet. In general, however, members of the SPL family are implicated in controlling plastochron setting (Schwarz et al., 2008; Wang et al., 2008; Leyser, 2009). *BT5* (At4g37610), which encodes a cytosolic protein of the BTB/TAZ family (Robert et al., 2009), was also one of the down-regulated genes; its function is unknown. MapMan analysis (Usadel et al., 2006) confirmed that genes controlled by EBE are mainly involved in lipid metabolism (lipid transfer proteins), cell wall modification, RNA regulation of transcription, and auxin metabolism (signal transduction; Supplemental Table S3).

Potential Regulatory Elements in Promoters of EBE Downstream Genes

Since EBE is an AP2/ERF transcription factor, we analyzed the 1-kb promoters of the 48 EBE-affected genes for the presence of cis-elements known to be targeted by AP2/ERFs (compare with Supplemental Table S4), using POBO (http://ekhidna.biocenter.helsinki.fi/poxo/pobo) and Expression Angler (http://bar.utoronto.ca/ntools/cgi-bin/BAR_Promomer.cgi; Kankainen and Holm, 2004; Toufighi et al., 2005), revealing a significant overrepresentation of the HvCBF2-binding site GTCGAC (Fig. 7A; Supplemental Table S4). While several promoters contain ERF-like binding sequences (such as *CIPK11*, *AtLTP6*, and *AtLTP12*), some others (*AtMYB60* and *AtXTH9*) did not and, therefore, might represent secondary downstream targets of EBE (Supplemental Table S4).

Tatematsu et al. (2005) previously searched for sequence motifs overrepresented in promoters of genes up- or down-regulated after main shoot decapitation and observed that promoters of down-regulated genes were enriched for the TATCC motif that resembles the sugar-repressive element (SRE), whereas promoters of up-regulated genes were enriched for GGCCCAWW (named Up1) and AAACCCTA (Up2) motifs. As EBE affects axillary bud outgrowth, we searched for SRE, Up1, and Up2 regulatory elements in 1-kb upstream regions of EBE-affected genes. We observed a significant overrepresentation of the SRE motif in promoters of the 34 down-regulated genes when compared with the Arabidopsis background data set (Fig. 7B). In Arabidopsis, the two TCP transcription factors BRC1 and BRC2 control shoot branching (Aguilar-Martínez et al., 2007; Finlayson, 2007; Martín-Trillo et al., 2011). POBO analysis indicated that the TCP-binding sites GGNCCCAC and G(T/C)GGNCCC (Kosugi and Ohashi, 2002; Welchen and Gonzalez, 2006; Martín-Trillo and Cubas, 2010) are overrepresented in the 1-kb promoters of the 48 EBE downstream genes (Fig. 7, C and D), suggesting that members of the TCP family, including BRC1, may act together with EBE to jointly regulate their expression.

DISCUSSION

Shoot branching is a finely regulated developmental process tuned by both endogenous and environmental cues (Wang and Li, 2008; Finlayson et al., 2010; Domagalska and Leyser, 2011). In many cases, newly formed axillary buds remain dormant for some time before growing out to form a branch. The shoot apex exerts an inhibitory effect on bud outgrowth, a phenomenon known as apical dominance (Shimizu-Sato and Mori, 2001). Apical dominance can be released by environmental and developmental signals (Shimizu-Sato and Mori, 2001; Dun et al., 2006).

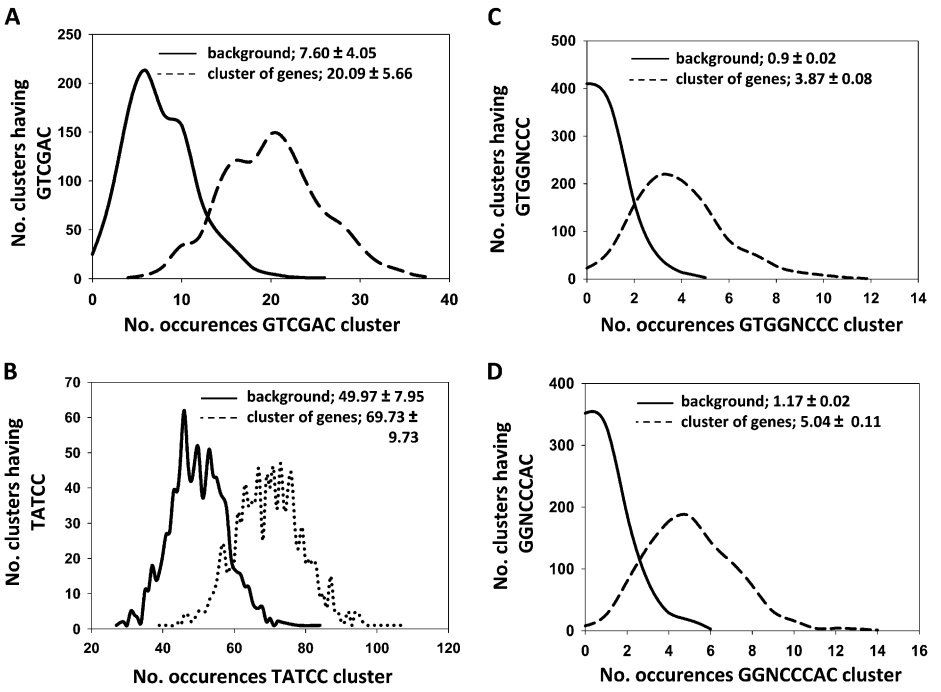

Figure 7. Overrepresentation analysis of cis-regulatory motifs in the promoters of early EBE target genes. A, Overrepresentation of the GTCGAC motif in the promoters of the 48 early target genes compared with the background. B, The TATCC motif (SRE) is more abundant in the promoters of the 34 down-regulated EBE early target genes than in the background data set. C and D, Overrepresentation of TCP target sites in the promoters of the 48 EBE downstream targets. All analyses were performed using the POBO program. Dashed lines indicate the occurrence of motifs in EBE downstream genes, and solid lines indicate the occurrence of motifs in the background data set.

Although various genes controlling shoot architecture have been reported, the underlying regulatory mechanisms, in particular those acting in the axillary bud itself, are currently not well understood. Here, we report that EBE, an ERF transcription factor of the AP2/ERF superfamily, has an impact on shoot architecture. As we show, the number of outgrowing buds is decreased in *EBE-RNAi* lines and increased in *EBE* overexpression lines compared with the wild type (Fig. 3, A and B). These differences cannot be attributed to potential differences in developmental speed, as RNAi lines never produced as many lateral branches as wild-type plants, even if they were grown until complete senescence. Similarly, *EBE* overexpressors consistently had higher numbers of lateral branches than wild-type plants even upon full senescence. Moreover, main stem decapitation rapidly (within 1 h) enhances *EBE* expression in axillary buds of wild-type plants (Fig. 5C). Of note, in estradiol-inducible *EBE* overexpression lines, *AtDRM1*, *AtDRM1 homolog* (At2g33830), and *MARD1/SAG102* (At3g63210) are remarkably down-regulated after *EBE* induction. These genes are also strongly down-regulated in buds that start to grow (*AtDRM1* and *AtDRM1 homolog*; Tatematsu et al., 2005). On the other hand, dormancy release occurs concomitant with the up-regulation of genes that function during G1-to-S-phase transition, such as D-type cyclins (*CYCD*; Shimizu-Sato and Mori, 2001; Horvath et al., 2003; Tatematsu et al., 2005). Of note, *CYCD3;3* is remarkably up-regulated after *EBE* induction. Furthermore, the promoters of *AtDRM1 homolog* and *MARD1* both contain the GTCGAC motif (HvCBF2-binding sequence), which is overrepresented in the promoters of the 48 EBE target genes (Fig. 7A). Similarly, the *AtDRM1* and *CYCD3;3* promoters contain GCCGAC and ATCGAC sequences, respectively, both of which are alternative sequences to GTCGAC with lower binding affinities (Xue, 2003). This result indicates that the above genes might be direct targets of EBE. In addition, we observed an overrepresentation of the SRE element, which was previously implicated in axillary bud outgrowth (Tatematsu et al., 2005), in the promoters of the 34 EBE down-regulated genes (Fig. 7B). Although binding of EBE to these motifs has not been tested experimentally yet, this result further supports the model that EBE is an important regulator of axillary bud outgrowth.

Although the altered branching pattern observed in *EBE*-modified plants may primarily be caused by direct effects on regulatory processes in axillary buds, the alternative possibility, that the developmental phenotype is at least partly caused by perturbed apical dominance, cannot be disregarded at present. Notably, *EBE* expression is widely detected in various plant tissues rather than being restricted to axillary buds only (Fig. 1). Thus, EBE might actually exert its role in different plant organs by affecting, for example, the function of phytohormones such as auxin, cytokinin, or strigolactones, or other unidentified long-distance signals. In agreement with this hypothesis, the primary shoot apex of *35S:EBE* and *EBE:RNAi* plants is often disorganized (Fig. 6C). Furthermore, ectopic overexpression of *EBE* triggers neoplastic capacity (Supplemental Fig. S1, A–C), indicating that auxin/cytokinin balance or signaling may be perturbed. The phenotype observed for *EBE* overexpression plants to some extent resembles that of the *altered meristem program1* mutant, which lacks apical dominance and has

an elevated cytokinin level (Chaudhury et al., 1993; Nogué et al., 2000). However, in *35S:EBE* plants, the branching phenotype may not be causally linked to an elevated cytokinin level. We observed a slightly earlier senescence in *35S:EBE* than in wild-type plants (data not shown), indicating that cytokinin level may be reduced rather than increased.

Most plant cells are totipotent. Totipotency requires the acquisition of stem cell potential (dedifferentiation) in response to proper stimuli and expressing this potential during subsequent morphogenesis (regeneration). During dedifferentiation, genome reprogramming occurs to establish a stem cell status, and subsequently, gene activity patterns change in a systematic manner while entering the regeneration phase (Sugiyama, 1999; Grafi, 2004). *EBE* is preferentially expressed during the S phase of the cell cycle (Fig. 1A) and is highly active in dividing cells (Fig. 1, A and B; Menges et al., 2003; Deeken et al., 2006; Sugimoto et al., 2010), indicating that it regulates the expression of genes important for cell proliferation. Thus, the pleiotropic phenotype induced by the ectopic expression of *EBE* may to some extent be caused by disconnecting the expression of its target genes from the regular developmental program. In addition, our experimental data suggest that elevated *EBE* expression in wounded and senescent leaf areas may affect stem cell potentiality and subsequent morphogenesis (regeneration). Notably, transcriptome profiling previously showed remarkable similarities between senescing and dedifferentiating protoplast cells, indicating that both cell states share common molecular characteristics (Damri et al., 2009; Grafi et al., 2011). Those authors proposed a model in which the response of plant cells to stress (which often triggers precocious senescence) converges on cellular dedifferentiation, which leads to a stem cell-like fate before cells adopt a new fate (Grafi et al., 2011). In accordance with this model, tissues phenotypically resembling green calli, or organ-like structures, regenerated from wounded sites or partially senesced tissues of *35S:EBE* plants (Supplemental Fig. S1, A–C). Worth mentioning is that *EBE* resembles the *WOUND-INDUCED DEDIFFERENTIATION1* (*WIND1*) gene and its close homologs *WIND2*, *WIND3*, and *WIND4*, all of which are induced by wounding and promote cell dedifferentiation in Arabidopsis (Iwase et al., 2011). However, a role in bud outgrowth and shoot branching was not reported for these other AP2/ERF transcription factors. Of note, the *WIND* genes encode group Ib AP2/ERF transcription factors, while EBE is a member of group Xa (Nakano et al., 2006).

It is well established that the SAM, along its radial axis, is organized into a central zone that includes a source of pluripotent stem cells as well as a peripheral zone in which appendages, including leaves and flowers, are generated (Dodsworth, 2009; Barton, 2010; Ha et al., 2010). Transgenic *EBE* plants showed altered SAM size, leaf initiation rate, phyllotaxy, and axillary bud formation and outgrowth. As shown in Figure 6C, the apical apex of *35S:EBE* plants can massively enlarge, indicating that *EBE* overexpression affects meristem maintenance. Moreover, *35S:EBE* plants develop buds in their cotyledonary nodes, which is normally not observed in wild-type plants. On the other hand, leaf primordia were initiated in some cases in *35S:EBE* plants but failed to develop further (Supplemental Fig. S6A), indicating that *EBE* overexpression perturbs peripheral organ development.

Previously, transcription factors of the TCP family, including BRC1 and BRC2 in Arabidopsis, were shown to play a critical role in shoot branching (Aguilar-Martínez et al., 2007; Finlayson, 2007; Martín-Trillo et al., 2011; Braun et al., 2012). Generally, loss of function of these transcription factors leads to increased branching, while overexpression leads to inhibition of bud outgrowth, identifying them as negative regulators of branching. In contrast, EBE, a member of the AP2/ERF transcription factor superfamily (Nakano et al., 2006), acts as a positive regulator of bud outgrowth and shoot branching (Fig. 3). Currently, the regulatory interplay between BRC1 (or BRC2) and EBE in the control of branch growth remains unknown. *BRC1* has been suggested to integrate endogenous and environmental signals to control bud outgrowth (Aguilar-Martínez et al., 2007). Class II TCPs, to which BRC1 belongs, have been proposed to repress organ growth by inhibiting cell proliferation at the G1-to-S transition (Martín-Trillo and Cubas, 2010; Aggarwal et al., 2011). *EBE* shows elevated expression during the S phase of the cell cycle and lower expression levels in the other phases (Fig. 1A; Menges et al., 2003). As TCP-binding sites are overrepresented in promoters of EBE downstream genes, their expression may be jointly regulated by both types of transcription factors. Future experiments will have to unravel the intricacies of the transcriptional control acting during dormancy breaking and bud outgrowth in more detail; the BRC1/BRC2 and EBE transcription factors are excellent starting points for achieving this goal.

MATERIALS AND METHODS

General

Standard molecular biological techniques were performed as described by Sambrook et al. (2001). DNA sequencing was achieved by AGOWA. Oligonucleotides were obtained from MWG Biotech. Unless indicated otherwise, chemicals were purchased from Roche, Merck, Invitrogen, Sigma-Aldrich, and Fluka. Molecular biology kits were obtained from Qiagen and Macherey-Nagel.

Databases and Biocomputational Tools

For sequence and expression analyses, the following databases and tools were used: eFP browser (http://bbc.botany.utoronto.ca/efp/cgi-bin/efpWeb.cgi); ExPASy (http://us.expasy.org/); Expression Angler (http://bar.utoronto.ca/ntools/cgi-bin/BAR_Promomer.cgi); Genevestigator (https://www.genevestigator.ethz.ch); National Center for Biotechnology Information (http://www.ncbi.nlm.nih.gov/); PLACE (http://www.dna.affrc.go.jp/PLACE/); PlnTFDB (http://plntfdb.bio.uni-potsdam.de/v3.0/); and The Arabidopsis Information Resource (http://www.arabidopsis.org/). Frequencies of motifs in EBE downstream genes were calculated using POBO (http://ekhidna.biocenter.helsinki.fi/poxo/pobo) on 1-kb promoter sequences of all 48 EBE-responsive genes (Table I) extracted from the

repository of The Arabidopsis Information Resource. For bootstrap analysis, the following parameters were used: number of pseudoclusters, 1,000; number of sequences in the pseudocluster, 48; promoter length, 1,000 bp.

Biological Material

All experiments were performed using Arabidopsis (*Arabidopsis thaliana*) ecotype Col-0. *Agrobacterium tumefaciens* strain GV3101 (pMP90) was used for Arabidopsis transformations. *Escherichia coli* strain DH5α (Stratagene) was employed for standard DNA work.

Growth Conditions

For tissue culture, Arabidopsis seeds were surface sterilized in 70% ethanol for 2 min and then in sterilization solution (20% sodium hypochlorite) for 20 min. After sterilization, the seeds were sown on one-half-strength MS medium (Murashige and Skoog, 1962) supplemented with 1% (w/v) Suc and appropriate antibiotics and solidified with 0.7% (w/v) phytoagar. After imbibition, the seeds were stratified at 4°C for 3 d. The seeds were germinated at 22°C under a 16-h-day (140 μmol m^{-2} s^{-1})/8-h-night regime. Two-week-old seedlings were carefully removed from plates and transplanted to soil in 6-cm pots (Einheitserde GS90; Gebrüder Patzer) or, if necessary, directly subjected to various treatments. Unless otherwise indicated, Arabidopsis plants were grown in controlled conditions in a growth chamber with a 16-h daylength provided by fluorescent light at 80 or 120 μmol m^{-2} s^{-1}, day/night temperatures of 20°C/16°C, and relative humidity of 60%/75% (long-day conditions). Short-day conditions were as follows: 8-h day (150 μmol m^{-2} s^{-1}), day/night temperatures of 20°C/18°C, and relative humidity of 60%/75%.

Constructs

35S:EBE

The *EBE* coding region (Arabidopsis Genome Initiative code At5g61890) was PCR amplified from Arabidopsis. Col-0 complementary DNA (cDNA) was inserted into pUni/V5-His-TOPO (Invitrogen) and, after sequence confirmation, cloned via the *Pme*I/*Pac*I sites into a modified pGreen0229 plant transformation vector (www.pgreen.ac.uk) containing a CaMV 35S promoter (Skirycz et al., 2006).

EBE-XVE

The *EBE* coding region was PCR amplified from Arabidopsis Col-0 cDNA using primers EBE-fwd-1 (5′-CTCGAGATGTATGGGAAGAGG-3′) and EBE-rev-1 (5′-ACTAGTTTAATATCCCGAATGAGG-3′). The amplified fragment was inserted into plasmid pCR-2.1-TOPO (Invitrogen) and subsequently fused via *Xho*I/*Spe*I sites into the pER8 vector (Zuo et al., 2000).

EBE-RNAi

An approximately 200-bp fragment of the *EBE* coding region (exon 2) was PCR amplified from Col-0 cDNA using primers EBE-fwd (5′-CACCGGAGAGGGTTCAGCTTGG-3′) and EBE-rev (5′-GTTGTAGCAGCAGTCGTAGTAC-3′). The PCR product was cloned into vector pENTR/D-TOPO of the Gateway system (Invitrogen). After sequencing, the *EBE* fragment was transferred to Gateway-compatible binary vector pBINAR-RNAi (kindly provided by Dr. Fernando Carrari, Max-Planck Institute of Molecular Plant Physiology) by *attL* × *attR* recombination, resulting in plasmid *EBE-RNAi*. The vector carries the CaMV 35S promoter upstream of the *EBE* silencing construct. After transformation into Arabidopsis, 25 independent kanamycin-resistant seedlings were chosen to test for reduced *EBE* transcript level using qRT-PCR.

$Prom_{EBE}$:GUS

An approximately 2-kb fragment upstream of the translation start codon of the *EBE* gene was PCR amplified from Arabidopsis Col-0 genomic DNA using primers EBE-GUS-fwd (5′-AAGCTTGACATATGGAGAAAGTGTCC-3′) and EBE-GUS-rev (5′-TCTAGATCCGAGGATCTACTTTTGC-3′). The promoter fragment was inserted into plasmid pCR-2.1-TOPO and subsequently fused via *Spe*I/*Xho*I (vector sites) to the *GUS* reporter gene in pGPTV-Kan (Becker et al., 1992), previously cut with *Xba*I/*Sal*I, resulting in plasmid *$Prom_{EBE}$:GUS*.

EBE T-DNA Insertion Line

An Arabidopsis line (SALK_000833) carrying a T-DNA insertion approximately 400 bp upstream of the *EBE* translation start codon (ATG) was obtained from the Nottingham Arabidopsis Stock Centre (http://arabidopsis.info/). Homozygous insertion lines were identified by PCR on genomic DNA. The approximate location of the T-DNA within the *EBE* gene was confirmed by PCR (Supplemental Fig. S3, A and B). The presence of the *EBE* wild-type allele was tested using primers EBE-F-promoter (5′-AAGCTTACCTGTCAACTTAGTTAGC-3′) and EBE-R-promoter (5′-TCTAGATCCGAGGATCTACTTTTGC-3′). The presence of the T-DNA insertion allele was tested using T-DNA left border primers (5′-GGCAATCAGCTGTTGCCCGTCTCACTGGTG-3′ and 5′-TGGTTCACGTAGTGGGCCATCG-3′) in combination with the EBE-R-promoter primer. *EBE* expression in the wild type and T-DNA insertion lines was tested by qRT-PCR.

Estradiol Induction Experiments

EBE-XVE and wild-type (control) seeds were cultured on MS agar plates at 22°C under a 16-h-day (140 μmol m^{-2} s^{-1})/8-h-night regime. After 3 weeks, seedlings were transferred to MS liquid medium while shaking. Sixteen hours later, 17-EST (Sigma-Aldrich) was added to the medium to a final concentration of 2 μM. Subsequently, whole shoots or rosette leaves were harvested at different time points after EST addition (30 min, 45 min, and 1, 4, 6, and 20 h).

GUS Assays

GUS activity was determined histochemically as described (Plesch et al., 2001). T2 and T3 plants were used for all studies. Infiltrated plants were incubated in GUS staining solution for 1 to 20 h at 37°C. For wounding experiments, mature leaves were injured with a needle. GUS staining was started 1 to 48 h after application of the wound stress. Plant material for microscopy was infiltrated and embedded in Technovit 7100 (Kulzer) as instructed by the manufacturer. Sections of 4-μm thickness were made on a Leica RM 2155 rotary microtome carrying a disposable Adams steel knife.

Expression Profiling by qRT-PCR

Total RNA extraction, cDNA synthesis, and qRT-PCR were performed as described previously (Caldana et al., 2007; Balazadeh et al., 2008). PCR was run on an ABI PRISM 7900HT sequence detection system (Applied Biosystems Applera).

Microarray Analysis

Three micrograms of quality-checked total RNA obtained from leaves of three biological replicates of *EBE-XVE* plants at time point 45 min were processed for use in Affymetrix ATH1 hybridizations. Labeling, hybridization, washing, staining, and scanning procedures were performed by an Affymetrix-authorized service provider (ATLAS Biolabs) as described in the Affymetrix technical manual. Raw data (CEL files) obtained from RNA hybridization experiments were normalized with the affyPLM package from the Bioconductor software project (Gentleman et al., 2004) using GCRMA, which employs the GC content of probes in normalization with robust multiple array average and gives one value for each probe set instead of keeping probe-level information (Wu et al., 2004). The transcriptional changes were determined by subtracting the normalized signal intensity of the control samples from that of induced samples. Expression data were submitted to the National Center for Biotechnology Information Gene Expression Omnibus repository (www.ncbi.nlm.nih.gov/geo/) under accession number GSE27855.

Callus Formation and Shoot and Root Regeneration

Leaf segments from seedlings were precultured on CIM (containing 2% Suc, 1 mg L^{-1} 2,4-dichlorophenoxyacetic acid, and 0.2 mg L^{-1} kinetin) for 4 d and then transferred to shoot-induction medium (containing 2% Suc, 1 mg L^{-1} benzylaminopurine, and 0.4 mg L^{-1} naphthalene acetic acid), root-induction medium (containing 2% Suc and 0.4 mg L^{-1} naphthalene acetic acid), or new CIM. Media were refreshed every 2 weeks.

Analysis of Shoot Branching

Shoot branches or axillary buds were analyzed using a binocular. Rosette leaf axils were examined individually beginning with the oldest one. Leaves

were removed successively after study so that the younger leaf axils became accessible. Lateral buds with at least 0.5 cm length were considered as lateral branches. Ten to 20 plants were analyzed in each experiment, and each experiment was performed at least twice.

Main Stem Decapitation

Prom$_{EBE}$:GUS seeds were cultured in one-half-strength MS medium in glass pots. The seeds were germinated at 22°C under a 16-h-day (140 μmol m^{-2} s^{-1})/8-h-night regime. Main stems were decapitated 4 to 7 d after bolting, at stem height of 2 to 5 cm, and when axillary buds were visible. GUS activity was analyzed 6 and 14 h after decapitation.

Decapitation-controlled expression of *EBE* was confirmed in wild-type Arabidopsis plants by qRT-PCR. Plants were grown in long-day conditions, and decapitation was done when the main stem was approximately 10 cm high. The five top axillary shoots were harvested at different time points (1, 6, 9, 15, and 24 h) after decapitation and mixed before analysis. The same procedure was applied for intact plants.

Scanning Electron Microscopy

Tissues were fixed in 4% formaldehyde in 0.07 M sodium phosphate/potassium phosphate buffer (pH 7.2) at 4°C for 4 to 16 h. Then, tissues were rinsed in sodium phosphate/potassium phosphate buffer for 1 h, dehydrated in a graded ethanol series, and critical point dried in vacuum. Samples were coated with gold/palladium and examined at an accelerating voltage of 10 kV with a high-resolution SEM LEO 1550 microscope (Carl Zeiss).

Supplemental Data

The following materials are available in the online version of this article.

Supplemental Figure S1. Neoplastic activity in *35S:EBE* plants.

Supplemental Figure S2. Phenotypic effects of enhanced *EBE* transcript level.

Supplemental Figure S3. Analysis of the *ebe-1D* mutant.

Supplemental Figure S4. Phenotype of *EBE-RNAi* lines.

Supplemental Figure S5. Leaf and cell sizes.

Supplemental Figure S6. Phenotype of SAM and *EBE* expression shown by GUS staining.

Supplemental Figure S7. Phenotype induced by estradiol-induced *EBE* overexpression.

Supplemental Table S1. Number of cauline leaf branches in transgenic lines compared with the wild type.

Supplemental Table S2. Length of primary inflorescences in transgenic and wild-type plants.

Supplemental Table S3. Overrepresentation analysis of the 48 genes rapidly responding to enhanced *EBE* expression.

Supplemental Table S4. Target DNA-binding sequences of AP2/ERF domain proteins in the promoters of EBE downstream genes.

Supplemental Table S5. Flowering time points in *EBE*-modified plants.

ACKNOWLEDGMENTS

We thank Eugenia Maximova for excellent microscopic assistance; Nooshin Omranian for help with statistical analyses; Josef Bergstein for photographic work; Karin Koehl and her colleagues for expert plant care; Fernando Carrari for providing pBINAR-RNAi vector; Erwan Michard for introducing M.M. to EBE; the anonymous reviewers for helpful comments on the manuscript; and the Nottingham Arabidopsis Stock Centre for providing seeds of the *ebe-1D* T-DNA insertion line.

Received January 9, 2013; accepted April 23, 2013; published April 24, 2013.

LITERATURE CITED

Aggarwal P, Padmanabhan B, Bhat A, Sarvepalli K, Sadhale PP, Nath U (2011) The TCP4 transcription factor of Arabidopsis blocks cell division in yeast at G1→S transition. Biochem Biophys Res Commun **410:** 276–281

Aguilar-Martínez JA, Poza-Carrión C, Cubas P (2007) *Arabidopsis BRANCHED1* acts as an integrator of branching signals within axillary buds. Plant Cell **19:** 458–472

Bainbridge K, Guyomarc'h S, Bayer E, Swarup R, Bennett M, Mandel T, Kuhlemeier C (2008) Auxin influx carriers stabilize phyllotactic patterning. Genes Dev **22:** 810–823

Bakan B, Hamberg M, Perrocheau L, Maume D, Rogniaux H, Tranquet O, Rondeau C, Blein J-P, Ponchet M, Marion D (2006) Specific adduction of plant lipid transfer protein by an allene oxide generated by 9-lipoxygenase and allene oxide synthase. J Biol Chem **281:** 38981–38988

Balazadeh S, Riaño-Pachón DM, Mueller-Roeber B (2008) Transcription factors regulating leaf senescence in *Arabidopsis thaliana*. Plant Biol (Stuttg) (Suppl 1) **10:** 63–75

Barton MK (2010) Twenty years on: the inner workings of the shoot apical meristem, a developmental dynamo. Dev Biol **341:** 95–113

Bayer EM, Bottrill AR, Walshaw J, Vigouroux M, Naldrett MJ, Thomas CL, Maule AJ (2006) Arabidopsis cell wall proteome defined using multidimensional protein identification technology. Proteomics **6:** 301–311

Becker D, Kemper E, Schell J, Masterson R (1992) New plant binary vectors with selectable markers located proximal to the left T-DNA border. Plant Mol Biol **20:** 1195–1197

Beveridge CA, Kyozuka J (2010) New genes in the strigolactone-related shoot branching pathway. Curr Opin Plant Biol **13:** 34–39

Boe A, Beck DL (2008) Yield components of biomass in switchgrass. Crop Sci **48:** 1306–1311

Bonser SP, Aarssen LW (2003) Allometry and development in herbaceous plants: functional responses of meristem allocation to light and nutrient availability. Am J Bot **90:** 404–412

Braun N, de Saint Germain A, Pillot JP, Boutet-Mercey S, Dalmais M, Antoniadi I, Li X, Maia-Grondard A, Le Signor C, Bouteiller N, et al (2012) The pea TCP transcription factor PsBRC1 acts downstream of strigolactones to control shoot branching. Plant Physiol **158:** 225–238

Caldana C, Scheible WR, Mueller-Roeber B, Ruzicic S (2007) A quantitative RT-PCR platform for high-throughput expression profiling of 2500 rice transcription factors. Plant Methods **3:** 7

Chaudhury AM, Letham S, Craig S, Dennis ES (1993) *amp1*: a mutant with high cytokinin levels and altered embryonic pattern, faster vegetative growth, constitutive photomorphogenesis and precocious flowering. Plant J **4:** 907–916

Che P, Lall S, Nettleton D, Howell SH (2006) Gene expression programs during shoot, root, and callus development in Arabidopsis tissue culture. Plant Physiol **141:** 620–637

Damri M, Granot G, Ben-Meir H, Avivi Y, Plaschkes I, Chalifa-Caspi V, Wolfson M, Fraifeld V, Grafi G (2009) Senescing cells share common features with dedifferentiating cells. Rejuvenation Res **12:** 435–443

Deeken R, Engelmann JC, Efetova M, Czirjak T, Müller T, Kaiser WM, Tietz O, Krischke M, Mueller MJ, Palme K, et al (2006) An integrated view of gene expression and solute profiles of *Arabidopsis* tumors: a genome-wide approach. Plant Cell **18:** 3617–3634

De Veylder L, Beeckman T, Beemster GTS, de Almeida Engler J, Ormenese S, Maes S, Naudts M, Van Der Schueren E, Jacqmard A, Engler G, et al (2002) Control of proliferation, endoreduplication and differentiation by the Arabidopsis E2Fa-DPa transcription factor. EMBO J **21:** 1360–1368

Devitt ML, Stafstrom JP (1995) Cell cycle regulation during growth-dormancy cycles in pea axillary buds. Plant Mol Biol **29:** 255–265

Dodsworth S (2009) A diverse and intricate signalling network regulates stem cell fate in the shoot apical meristem. Dev Biol **336:** 1–9

Doebley J, Stec A, Hubbard L (1997) The evolution of apical dominance in maize. Nature **386:** 485–488

Domagalska MA, Leyser O (2011) Signal integration in the control of shoot branching. Nat Rev Mol Cell Biol **12:** 211–221

Doust A (2007) Architectural evolution and its implications for domestication in grasses. Ann Bot (Lond) **100:** 941–950

Dun EA, Ferguson BJ, Beveridge CA (2006) Apical dominance and shoot branching: divergent opinions or divergent mechanisms? Plant Physiol **142:** 812–819

Ferguson BJ, Beveridge CA (2009) Roles for auxin, cytokinin, and strigolactone in regulating shoot branching. Plant Physiol **149:** 1929–1944

Finlayson SA (2007) Arabidopsis Teosinte Branched1-like 1 regulates axillary bud outgrowth and is homologous to monocot Teosinte Branched1. Plant Cell Physiol **48:** 667–677

Finlayson SA, Krishnareddy SR, Kebrom TH, Casal JJ (2010) Phytochrome regulation of branching in Arabidopsis. Plant Physiol **152:** 1914–1927

Foo E, Bullier E, Goussot M, Foucher F, Rameau C, Beveridge CA (2005) The branching gene *RAMOSUS1* mediates interactions among two novel signals and auxin in pea. Plant Cell **17:** 464–474

García del Moral MB, García del Moral LF (1995) Tiller production and survival in relation to grain yield in winter and spring barley. Field Crops Res **44:** 85–93

Gentleman RC, Carey VJ, Bates DM, Bolstad B, Dettling M, Dudoit S, Ellis B, Gautier L, Ge Y, Gentry J, et al (2004) Bioconductor: open software development for computational biology and bioinformatics. Genome Biol **5:** R80

Grafi G (2004) How cells dedifferentiate: a lesson from plants. Dev Biol **268:** 1–6

Grafi G, Chalifa-Caspi V, Nagar T, Plaschkes I, Barak S, Ransbotyn V (2011) Plant response to stress meets dedifferentiation. Planta **233:** 433–438

Grbic V (2005) Comparative analysis of axillary and floral meristem development. Can J Bot **83:** 343–349

Ha CM, Jun JH, Fletcher JC (2010) Shoot apical meristem form and function. Curr Top Dev Biol **91:** 103–140

Han P, Li Q, Zhu Y-X (2008) Mutation of *Arabidopsis* BARD1 causes meristem defects by failing to confine WUSCHEL expression to the organizing center. Plant Cell **20:** 1482–1493

Hayward A, Stirnberg P, Beveridge C, Leyser O (2009) Interactions between auxin and strigolactone in shoot branching control. Plant Physiol **151:** 400–412

He Y, Gan S (2004) A novel zinc-finger protein with a proline-rich domain mediates ABA-regulated seed dormancy in Arabidopsis. Plant Mol Biol **54:** 1–9

Hong SY, Kim OK, Kim SG, Yang MS, Park CM (2011) Nuclear import and DNA binding of the ZHD5 transcription factor is modulated by a competitive peptide inhibitor in Arabidopsis. J Biol Chem **286:** 1659–1668

Horvath DP, Anderson JV, Chao WS, Foley ME (2003) Knowing when to grow: signals regulating bud dormancy. Trends Plant Sci **8:** 534–540

Iwase A, Mitsuda N, Koyama T, Hiratsu K, Kojima M, Arai T, Inoue Y, Seki M, Sakakibara H, Sugimoto K, et al (2011) The AP2/ERF transcription factor WIND1 controls cell dedifferentiation in Arabidopsis. Curr Biol **21:** 508–514

Kader J-C (1996) Lipid transfer proteins in plants. Annu Rev Plant Physiol Plant Mol Biol **47:** 627–654

Kankainen M, Holm L (2004) POBO, transcription factor binding site verification with bootstrapping. Nucleic Acids Res **32:** W222–W229

Kebrom TH, Burson BL, Finlayson SA (2006) Phytochrome B represses *Teosinte Branched1* expression and induces sorghum axillary bud outgrowth in response to light signals. Plant Physiol **140:** 1109–1117

Kosugi S, Ohashi Y (1997) PCF1 and PCF2 specifically bind to *cis* elements in the rice proliferating cell nuclear antigen gene. Plant Cell **9:** 1607–1619

Kosugi S, Ohashi Y (2002) DNA binding and dimerization specificity and potential targets for the TCP protein family. Plant J **30:** 337–348

Kwon H-K, Yokoyama R, Nishitani K (2005) A proteomic approach to apoplastic proteins involved in cell wall regeneration in protoplasts of Arabidopsis suspension-cultured cells. Plant Cell Physiol **46:** 843–857

Leyser O (2009) The control of shoot branching: an example of plant information processing. Plant Cell Environ **32:** 694–703

Li CJ, Guevara E, Herrera J, Bangerth F (1995) Effect of apex excision and replacement by 1-naphthylacetic acid on cytokinin concentration and apical dominance in pea plants. Physiol Plant **94:** 465–469

Martín-Trillo M, Cubas P (2010) TCP genes: a family snapshot ten years later. Trends Plant Sci **15:** 31–39

Martín-Trillo M, Grandío EG, Serra F, Marcel F, Rodríguez-Buey ML, Schmitz G, Theres K, Bendahmane A, Dopazo H, Cubas P (2011) Role of tomato *BRANCHED1*-like genes in the control of shoot branching. Plant J **67:** 701–714

Mayer KF, Schoof H, Haecker A, Lenhard M, Jürgens G, Laux T (1998) Role of WUSCHEL in regulating stem cell fate in the Arabidopsis shoot meristem. Cell **95:** 805–815

McSteen P, Leyser O (2005) Shoot branching. Annu Rev Plant Biol **56:** 353–374

Menges M, de Jager SM, Gruissem W, Murray JAH (2005) Global analysis of the core cell cycle regulators of Arabidopsis identifies novel genes, reveals multiple and highly specific profiles of expression and provides a coherent model for plant cell cycle control. Plant J **41:** 546–566

Menges M, Hennig L, Gruissem W, Murray JAH (2003) Genome-wide gene expression in an Arabidopsis cell suspension. Plant Mol Biol **53:** 423–442

Mizukami Y, Fischer RL (2000) Plant organ size control: AINTEGUMENTA regulates growth and cell numbers during organogenesis. Proc Natl Acad Sci USA **97:** 942–947

Mündermann L, Erasmus Y, Lane B, Coen E, Prusinkiewicz P (2005) Quantitative modeling of Arabidopsis development. Plant Physiol **139:** 960–968

Murashige T, Skoog F (1962) A revised medium for rapid growth and bioassays with tobacco tissue cultures. Physiol Plant **15:** 473–497

Nakano T, Suzuki K, Fujimura T, Shinshi H (2006) Genome-wide analysis of the ERF gene family in Arabidopsis and rice. Plant Physiol **140:** 411–432

Nogué F, Grandjean O, Craig S, Dennis S, Chaudhury M (2000) Higher levels of cell proliferation rate and cyclin *CycD3* expression in the Arabidopsis *amp1* mutant. Plant Growth Regul **32:** 267–273

Plesch G, Ehrhardt T, Mueller-Roeber B (2001) Involvement of TAAAG elements suggests a role for Dof transcription factors in guard cell-specific gene expression. Plant J **28:** 455–464

Reinhardt D, Kuhlemeier C (2002) Plant architecture. EMBO Rep **3:** 846–851

Renton M, Hanan J, Ferguson BJ, Beveridge CA (2012) Models of long-distance transport: how is carrier-dependent auxin transport regulated in the stem? New Phytol **194:** 704–715

Robert HS, Quint A, Brand D, Vivian-Smith A, Offringa R (2009) BTB and TAZ domain scaffold proteins perform a crucial function in Arabidopsis development. Plant J **58:** 109–121

Rubin G, Tohge T, Matsuda F, Saito K, Scheible WR (2009) Members of the LBD family of transcription factors repress anthocyanin synthesis and affect additional nitrogen responses in *Arabidopsis*. Plant Cell **21:** 3567–3584

Sambrook J, Fritsche EF, Maniatis T (2001) Molecular Cloning: A Laboratory Manual, Ed 3. Cold Spring Harbor Laboratory Press, Cold Spring Harbor, NY

Schwarz S, Grande AV, Bujdoso N, Saedler H, Huijser P (2008) The microRNA regulated SBP-box genes SPL9 and SPL15 control shoot maturation in Arabidopsis. Plant Mol Biol **67:** 183–195

Sena G, Wang X, Liu HY, Hofhuis H, Birnbaum KD (2009) Organ regeneration does not require a functional stem cell niche in plants. Nature **457:** 1150–1153

Shimizu S, Mori H (1998) Analysis of cycles of dormancy and growth in pea axillary buds based on mRNA accumulation patterns of cell cycle-related genes. Plant Cell Physiol **39:** 255–262

Shimizu-Sato S, Mori H (2001) Control of outgrowth and dormancy in axillary buds. Plant Physiol **127:** 1405–1413

Skirycz A, Reichelt M, Burow M, Birkemeyer C, Rolcik J, Kopka J, Zanor MI, Gershenzon J, Strnad M, Szopa J, et al (2006) DOF transcription factor AtDof1.1 (OBP2) is part of a regulatory network controlling glucosinolate biosynthesis in Arabidopsis. Plant J **47:** 10–24

Stafstrom JP, Ripley BD, Devitt ML, Drake B (1998) Dormancy-associated gene expression in pea axillary buds: cloning and expression of *PsDRM1* and *PsDRM2*. Planta **205:** 547–552

Sugimoto K, Jiao Y, Meyerowitz EM (2010) Arabidopsis regeneration from multiple tissues occurs via a root development pathway. Dev Cell **18:** 463–471

Sugiyama M (1999) Organogenesis *in vitro*. Curr Opin Plant Biol **2:** 61–64

Sussex IM, Kerk NM (2001) The evolution of plant architecture. Curr Opin Plant Biol **4:** 33–37

Tanaka M, Takei K, Kojima M, Sakakibara H, Mori H (2006) Auxin controls local cytokinin biosynthesis in the nodal stem in apical dominance. Plant J **45:** 1028–1036

Tatematsu K, Ward S, Leyser O, Kamiya Y, Nambara E (2005) Identification of *cis*-elements that regulate gene expression during initiation of axillary bud outgrowth in Arabidopsis. Plant Physiol **138:** 757–766

Toufighi K, Brady SM, Austin R, Ly E, Provart NJ (2005) The Botany Array Resource: e-northerns, expression angling, and promoter analyses. Plant J **43:** 153–163

Usadel B, Nagel A, Steinhauser D, Gibon Y, Bläsing OE, Redestig H, Sreenivasulu N, Krall L, Hannah MA, Poree F, et al (2006) PageMan: an interactive ontology tool to generate, display, and annotate overview graphs for profiling experiments. BMC Bioinformatics **7:** 535

Wang J-W, Schwab R, Czech B, Mica E, Weigel D (2008) Dual effects of *miR156*-targeted SPL genes and CYP78A5/KLUH on plastochron length and organ size in *Arabidopsis thaliana*. Plant Cell **20:** 1231–1243

Wang Y, Li J (2006) Genes controlling plant architecture. Curr Opin Biotechnol **17:** 123–129

Wang Y, Li J (2008) Molecular basis of plant architecture. Annu Rev Plant Biol **59:** 253–279

Welchen E, Gonzalez DH (2006) Overrepresentation of elements recognized by TCP-domain transcription factors in the upstream regions of nuclear genes encoding components of the mitochondrial oxidative phosphorylation machinery. Plant Physiol **141:** 540–545

Wu G, Poethig RS (2006) Temporal regulation of shoot development in *Arabidopsis thaliana* by *miR156* and its target *SPL3*. Development **133:** 3539–3547

Wu Z, Irizarry RA, Gentleman R, Martinez-Murillo F, Spencer F (2004) A model-based background adjustment for oligonucleotide expression arrays. J Am Stat Assoc **99:** 909–917

Xue GP (2003) The DNA-binding activity of an AP2 transcriptional activator HvCBF2 involved in regulation of low-temperature responsive genes in barley is modulated by temperature. Plant J **33:** 373–383

Yeats TH, Rose JKC (2008) The biochemistry and biology of extracellular plant lipid-transfer proteins (LTPs). Protein Sci **17:** 191–198

Zhao DL, Atlin GN, Bastiaans L, Spiertz JHJ (2006) Developing selection protocols for weed competitiveness in aerobic rice. Field Crops Res **97:** 272–285

Zimmermann P, Hirsch-Hoffmann M, Hennig L, Gruissem W (2004) GENEVESTIGATOR: Arabidopsis microarray database and analysis toolbox. Plant Physiol **136:** 2621–2632

Zuo J, Niu QW, Chua NH (2000) An estrogen receptor-based transactivator XVE mediates highly inducible gene expression in transgenic plants. Plant J **24:** 265–273